JBC

Manuscript Title:	Disruption of the cell surface glycoprotein CUB domain containing protein 1 (CDCP1) inhibits Epidermal Growth Factor Receptor-mediated cell migration
Manuscript No:	JBC/2011/335448 [R1]
Manuscript Type:	Regular Paper
Date Submitted by the Author:	25 Jan 2012
Complete List of Authors:	Ying Dong, Yaowu He, Leonore de Boer, M Sharon Stack, John W Lumley, Judith A Clements, and John D Hooper
Keywords:	Cell biology; Cell migration; Epidermal growth factor receptor (egfr); Ovarian cancer ; Protein structure; CDCP1

JBC

The cell surface glycoprotein CUB domain containing protein 1 (CDCP1) contributes to Epidermal Growth Factor Receptor-mediated cell migration

Ying Dong[‡], Yaowu He[§], Leonore de Boer[‡], M. Sharon Stack[¶1], John W. Lumley[‖], Judith A. Clements[‡] and John D. Hooper[§2]

Running Title: CDCP1 in EGFR-induced cell migration

[‡]Cancer Research Program, Institute of Health and Biomedical Innovation, Queensland University of Technology, Kelvin Grove, Queensland 4059, Australia; [§]Mater Medical Research Institute, South Brisbane, Queensland 4101, Australia; [¶]Department of Pathology and Anatomical Sciences, University of Missouri, Columbia, Missouri, 65212; [‖]Wesley Medical Centre, Auchenflower, Queensland 4066, Australia.

[1]Current address: Department of Chemistry and Biochemistry, Harper Cancer Research Institute, University of Notre Dame, Notre Dame, Indiana 46556.
[2]To whom correspondence should be addressed. Tel.: 61-7-3163-2555; Fax: 61-7-3163-2550;
E-mail: jhooper@mmri.mater.org.au

Keywords: CDCP1, EGF, EGFR, ovarian cancer.

Background: Epidermal growth factor (EGF) activates EGF receptor (EGFR) to promote cell migration and cancer.
Results: EGF/EGFR upregulates the cell surface glycoprotein CDCP1 and blockade of CDCP1 reduces EGF/EGFR-induced migration of ovarian cancer cells lines. CDCP1 is expressed by ovarian tumors.
Conclusion: CDCP1 contributes to EGF/EGFR-induced cell migration.
Significance: Targeting of CDCP1 may be a rational approach to inhibit cancers mediated by EGFR.

Epidermal growth factor (EGF) activation of the EGF receptor (EGFR) is an important mediator of cell migration and aberrant signaling via this system promotes a number of malignancies including ovarian cancer. We have identified the cell surface glycoprotein CDCP1 as a key regulator of EGF/EGFR-induced cell migration. We show that signaling via EGF/EGFR induces migration of ovarian cancer Caov3 and OVCA420 cells with concomitant upregulation of CDCP1 mRNA and protein. Consistent with a role in cell migration CDCP1 relocates from cell-cell junctions to punctate structures on filopodia following activation of EGFR. Significantly, disruption of CDCP1, either by silencing or the use of a function blocking antibody, efficiently reduces EGF/EGFR-induced cell migration of Caov3 and OVCA420 cells. We also show that upregulation of CDCP1 is inhibited by pharmacological agents blocking ERK but not Src signaling indicating that the

JBC

RAS/RAF/MEK/ERK pathway is required downstream of EGF/EGFR to induce increased expression of CDCP1. Our immunohistochemical analysis of benign, primary and metastatic serous epithelial ovarian tumors demonstrates that CDCP1 is expressed during progression of this cancer. These data highlight a novel role for CDCP1 in EGF/EGFR-induced cell migration and indicate that targeting of CDCP1 may be a rational approach to inhibit progression of cancers driven by EGFR signaling including those resistant to anti-EGFR drugs because of activating mutations in the RAS/RAF/MEK/ERK pathway.

Epidermal growth factor receptor (EGFR) is a receptor tyrosine kinase consisting of an extracellular ligand-binding domain, a membrane spanning region and a cytoplasmic tail containing a kinase domain and docking sites for signaling effectors and modulators (1, 2). Ligand mediated activation of EGFR requires binding, by one of at least six growth factors including epidermal growth factor (EGF), to the receptor extracellular domain (3, 4) which initiates autophosphorylation of specific receptor cytoplasmic tyrosine residues, including tyrosine 1068 (Y1068) (5). This triggers further signaling events, including activation of RAS/RAF/MEK/ERK (6, 7) and Src family kinase (SFK) (8-13) pathways, that promote a range of cellular processes including migration (14-16).

As with other mediators of migration, EGFR activation alters cellular plasticity to promote the transition from a morphology where cells are in intimate contact with neighbors and substratum, to an elongated, spindle shape associated with increased ability to migrate and invade into surrounding matrix (17-19). In a range of cell lines EGF/EGFR-mediated migration is accompanied by a so-called epithelial to mesenchymal transition (EMT) involving loss of expression of proteins necessary for maintenance of epithelial phenotypes, such as E-cadherin (20, 21), as well as augmented expression of proteins associated with mesenchymal phenotypes including N-cadherin (18, 22) and vimentin (23).

In physiological settings EGFR-mediated cell migration is tightly regulated to mediate normal development and homeostasis (24). However, in disease states, such as cancer, elevated EGFR signaling, either via activating mutations or increased expression, promotes aberrant cell migration. Interestingly, although this inappropriate activation of EGFR is a known promoter of malignancies of the lung, colon, pancreas, breast, head and neck and ovary (25) and targeting this receptor has shown much promise in preclinical settings, anti-EGFR drugs have been largely ineffective for the treatment of each of these cancers except non-small cell lung cancer (25, 26). The lack of efficacy of EGFR inhibition alone is due in part to drug resistance resulting from mutations in downstream signaling effectors such as RAS and RAF, or activation of other receptors including IGF-1R and Met (25, 26).

Recently the cell surface glycoprotein CUB domain containing protein 1 (CDCP1, also named SIMA135, gp140, Trask and CD318 (27-30)) has emerged as a promoter of cell migration *in vitro* and cancer cell dissemination in animal models (31, 32). For example, CDCP1 promotes *in vitro* migration and peritoneal dissemination of scirrhous gastric carcinoma cell lines (33) as well

JBC

as *in vitro* migration of pancreatic cancer cells (34). In addition, antibody targeting of CDCP1 inhibits prostate cancer cell migration and invasion *in vitro* and metastasis in a mouse xenograft model (35). Antibody based disruption of CDCP1 function has also been effective at blocking *in vivo* dissemination of a highly metastatic prostate cancer PC3 cell variant and HeLa and HEK293 cells ectopically expressing CDCP1 (36, 37). The mechanisms regulating CDCP1 in cell migration have been largely unexplored although recently this protein was shown to be regulated by hypoxia-inducible factor (HIF) 1α and 2α and to play a critical role in kidney cancer cell migration (38).

In this study we have used EGF/EGFR responsive epithelial ovarian cancer cell lines to explore the role of CDCP1 in EGFR-induced cell migration. We demonstrate that CDCP1 mRNA expression is upregulated by EGF/EGFR signaling via a pathway that involves the activity of ERK but not Src. We also show that antibody and shRNA-mediated disruption of CDCP1 efficiently block EGF/EGFR-induced cell migration. Our immunohistochemical analysis demonstrates that CDCP1 is expressed during ovarian cancer progression. Targeting of CDCP1 may be a rational approach to inhibit malignancies, such as ovarian cancer, that are driven by EGF/EGFR.

EXPERIMENTAL PROCEDURES

Antibodies and reagents–Antibodies were from the following suppliers: rabbit polyclonal antibody against unspecified C-terminal residues of CDCP1 (#4115 used in Western blot and immunohistochemical analyses), rabbit anti-pEGFR-Y1068, mouse anti-EGFR, rabbit anti-pSrc-Y416, mouse anti-Src, mouse anti-pMAPK/p44/42 (pERK1/2-Y202/204) and rabbit anti-ERK1/2 (Cell Signaling Technology, Quantum Scientific, Murarrie, Australia); monoclonal anti-glyceraldehyde-3-phosphate dehydrogenase (GAPDH) antibody and anti-mouse immunoglobulin (IgG) from Sigma (Castle Hill, Australia); monoclonal anti-E-cadherin and anti-N-cadherin antibodies and goat anti-mouse Alexa Fluor 488 antibody (Invitrogen, Mount Waverley, Australia); IRDye 680 or 800 conjugated mouse or rabbit IgG (LI-COR Biosciences, Lincoln, NE, USA); anti-CDCP1 monoclonal antibody 10D7 (used for confocal microscopy analysis and cell migration assays) was previously described (39). Alexa Fluor 568 phalloidin and 4'-6-diamidino-2-phenylindole (DAPI) were from Invitrogen, and Complete EDTA-free protease inhibitor cocktail was from Roche Applied Sciences (Castle Hill, Australia). EGFR antagonist AG1478, SFK selective inhibitor SU6656 and ERK inhibitor U0126 were from Sigma. All other reagents were from Sigma except where noted.

Cell lines, cell culture and treatment–The ovarian cancer cell lines OV90, Caov3 and SKOV-3, and a normal fibroblast cell line NFF1 were purchased from American Type Culture Collection (Manassas, VA). PEO1, PEO4, PEO14 and OAW42 epithelial ovarian cancer cell lines were described previously (40). OVCA420 and OVCA432 epithelial ovarian cancer cell lines (41) were kindly provided by Samuel Mok (University of Texas MD Anderson Cancer Center, Houston, TX). The OVMZ-6 cell line (42) was a kind gift from Viktor Magdolen (Technical University of Munich, Munich, Germany). All cell lines were cultured in RPMI 1640 media with 10% fetal calf serum (FCS) and penicillin (100 units/ml) and

JBC

streptomycin (100 units/ml) except for OVMZ-6 which were cultured in DMEM containing 10% FCS, penicillin (100 units/ml) and streptomycin (100 units/ml), 2 mM sodium pyruvate and L-glutamine (42). For treatments with pharmacological agents, cells were cultured until 60% confluent then washed twice with PBS before growth in serum free media (SFM) for 24 h before treatment with 0.1% DMSO, 0.1% DMSO with EGF (30 ng/ml), or 0.1% DMSO with EGF (30 ng/ml) and AG1478 (20 μM), SU6656 (10 μM) or U0126 (10 μM) for 0.2 and 24 h. For antibody treatments, cells were cultured as above followed by treatment with control IgG (20 μg/ml), EGF (30 ng/ml) and control IgG, or EGF (30 ng/ml) and CDCP1 function blocking antibody 10D7 (20 μg/ml).

RNA extraction and quantitative reverse transcription-PCR (RT-PCR)–Total RNA extraction and cDNA synthesis were performed as described previously (43). Briefly, total RNA was extracted using Trizol reagent (Invitrogen) followed by treatment with DNase I (Invitrogen), and 2 μg RNA was reverse-transcribed using a Superscript III reverse transcriptase kit (Invitrogen). Quantitative-RT-PCR was performed on a Rotor-Gene cycler (Qiagen, Doncaster, Australia) with *CDCP1* specific primers 5′-AATCTACGTGGTTGACTTGAGTAA-3′ and 5′-CCACATTCATCCACAGACG-3′ incorporating SYBR green (Takara, Tokyo, Japan). *CDCP1* expression was normalized to *HPRT1* (primers: forward, 5′-TGAACGTCTTGCTCGAGATGTG-3′ and reverse, 5′-CCAGCAGGTCAGCAAAGAATTT-3′). The ΔC_T method (44) was used to determine fold change from 3 separate experiments with triplicate wells per experiment.

Cell lysis and Western blot analysis–Whole cell lysates were collected in a buffer containing Complete protease inhibitor cocktail (1×), 2 mM sodium vanadate, 10 mM sodium fluoride, 50 mM Tris-HCl (pH 7.4), NaCl (150 mM) and CHAPS (1%). Protein concentration was determined by microbicinchoninic acid assay (Thermo Scientific). Cell lysates (20 μg) were separated by SDS-PAGE under reducing conditions, transferred to nitrocellulose membranes, and blocked in Odyssey blocking buffer (LI-COR® Biosciences). Membranes were incubated with primary antibodies diluted in blocking buffer overnight at 4ºC, washed with tris-buffered saline containing 0.05% Tween-20, and then incubated with secondary IRDye 680 or 800 conjugated mouse or rabbit IgG as appropriate. Images were generated and densitometry analysis was performed using the Odyssey system and software (LI-COR Biosciences).

Phase contrast and time-lapse images–Bright field images were captured using a phase contrast microscope and a digital camera (10 × objective, Nikon Eclipse TE2000-U, Nikon, Japan) and V++ software. Time lapse images were captured every 15 min up to 24 h using a Leica AF-1600 wide-field microscope and system software (Leica Microsystems, Sydney, Australia). Cell scattering was measured as the distance between cell nuclei in 3 independent experiments using InDesign software (Adobe, Adobe Systems Pty Ltd, Chatswood, Australia). For cells silenced for CDCP1, measurements were performed from images acquired from the Nikon Eclipse system on 200 pairs of cells from 10 randomly selected

JBC

fields per treatment group. For cells treated with anti-CDCP1 antibody 10D7 or control IgG, measurements were performed from time lapse images acquired on the Leica AF-1600 system on at least 80 individual randomly selected cells per treatment group.

Confocal microscopy analysis–Cells were grown in serum containing media on sterile cover-slips until 60% confluent. The cells were then grown in serum free media for a further 24 h then either left untreated or treated with EGF (30 ng/ml) for 24 h. After washes with PBS, cells were fixed (4% (w/v) paraformaldehyde in PBS), permeabilized (0.5% (v/v) Triton X-100 in PBS) and blocked (5% (w/v) BSA in PBS) then incubated with mouse monoclonal anti-CDCP1 antibody 10D7 (dilution 1:200 (v/v) in 1% BSA/PBS) at room temperature for 2 h. After washes, cells were incubated with a mouse Alexa Fluor 488 conjugated secondary antibody, Alexa Fluor 568 phalloidin and DAPI. Images were acquired using a Leica-TCS SP5 confocal microscope (63 × oil immersion objective lens).

Lentiviral shRNA gene silencing–CDCP1 expression was suppressed as previously described (45). Briefly, to generate lentivirus a CDCP1 pLKO.1 lentiviral shRNA knock-down construct (OpenBiosystems, Millennium Science, Surrey Hills, Australia) or a control scramble shRNA construct (Addgene, Cambridge, MA) was transfected into HEK293T cells together with packaging plasmids (pCMV-VSVG and pCMV-dR8.2-dvpr) using Lipofectamine 2000 (Invitrogen). Filtered conditioned media was used to sequentially infect target cells in the presence of 8 μg/ml of hexadimethrine bromide. Polyclonal pools of stably infected cells were selected in puromycin (2 μg/ml) containing medium for 1 week.

Immunohistochemistry–Paraffin-embedded tissue sections (4 μm) were from benign serous adenomas (n = 3), primary serous tumors (n = 3) and serous metastases (n = 3). The source of these tissues was described previously (43) and each was used with institutional ethics approval (Queensland University of Technology certificate no. 080000213) and informed patient consent. Immunohistochemistry was performed as previously described (40). Briefly, sections (4 μm) were deparaffinized in xylene and rehydrated followed by antigen retrieval with microwave heat treatment in 10 mM citric acid (pH 6.0). Sections were incubated overnight at 4°C with a rabbit anti-CDCP1-C-terminal antibody (1:100 in 1% (w/v) BSA in PBS) or rabbit IgG as negative control (Dako, Campbellfield, Australia). Signal was detected using the EnVision™ peroxidase system (Dako) and sections were counterstained with Gill's hematoxylin. Staining was visualized using an Olympus BX41 microscope (Olympus, Japan) and photographed with a Qimaging digital camera (MicroPublisher 3.3RTV) and associated software (QCapture Pro 6.0, Burnaby BC, Canada). Images were processed using Adobe Photoshop CS3 and displayed using CorelDraw14 (Corel Pty Ltd, Sydney, Australia).

Statistical analysis–One-tailed Student's t-tests were performed for statistical analysis. *P* values with a 95% confidence interval were obtained from at least 3 independent experiments using GraphPad Prism (GraphPad Software, Inc, La Jolla, CA). A P value < 0.05 was considered to be significant.

JBC

RESULTS

CDCP1 is upregulated by the EGF/EGFR signaling axis–To identify cell lines suitable for examination of the role of CDCP1 in EGF/EGFR-mediated cell migration, we first analyzed the expression of CDCP1 in 10 epithelial ovarian cancer derived cell lines. Anti-CDCP1 Western blot analysis was performed on lysates from cells cultured in serum containing media. CDCP1 is produced as a 135 kDa cell surface protein (28) that is proteolytically processed in a range of cultured cell lines (29, 44) as well as in *in vivo* settings (29, 37) to a 70 kDa cell retained form. As shown in Figure 1A, 70 and 135 kDa CDCP1 species were most highly expressed by OVCA420 cells with high relative expression of these species also apparent in OVCA432, PEO1 and PEO4 cells. Lower level expression of both bands was also apparent in OV90 and PEO14 cells while the 135 kDa band was apparent in OAW42 and SKOV-3 cells (Fig 1A). Caov3 cells expressed the 135 kDa band at high levels with much lower levels of 70 kDa CDCP1 generated by this cell line. OVMZ-6 cells were the only ovarian cancer line that did not express CDCP1.

A subset of the CDCP1 expressing cell lines (Caov3, OVCA420, OVCA432, PEO4) were next evaluated for the ability to respond to EGF stimulation. This was performed by Western blot analysis for phosphorylated EGFR-Y1068, a site that is phosphorylated by Jak2 to provide a docking site for Grb2 and activation of MAP kinases (46). In this and all subsequent experiments the effects of EGF stimulation were maximised by growth of cell lines in serum free media for 24 h before EGF stimulation. As shown in Figure 1B, EGF induced rapid phosphorylation of EGFR in each cell line and this was sustained for at least 1 h.

The effect of EGF signaling on CDCP1 expression was analyzed at mRNA and protein levels in two of the EGF responsive cell lines, Caov3 and OVCA420. Quantitative real-time RT-PCR analysis was performed on total RNA isolated from cells treated with EGF for 0.2 and 24 h. As shown in Figure 2A, while EGF had no effect on *CDCP1* mRNA levels at 0.2 h, it induced a greater than 2 fold increase in expression in both cell lines at 24 h.

Consistent data showing EGF-induced upregulation of CDCP1 were obtained at the protein level. In these experiments cells were serum starved for 24 h then stimulated with EGF for 0.1, 0.2, 0.5, 1, 8 and 24 h. In control experiments cells were treated with the potent and selective EGFR inhibitor AG1478 (47). As shown in Figure 2B (left), EGF induced an approximately 2.5 fold increase in expression of 135 kDa CDCP1 in Caov3 cells within 1 h and this was sustained up to 24 h. AG1478 treatment blocked this induction indicating that EGF-induced upregulation of CDCP1 was mediated by EGFR. In contrast with OVCA420 cells grown in serum containing media, which generated abundant levels of 70 kDa CDCP1 (Fig 1A), these cells grown in serum free media expressed very low levels of this species and like the Caov3 line, 70 kDa CDCP1 was not induced by EGF (Fig 2B). While it is clear that CDCP1 can undergo proteolytic conversion from 135 to 70 kDa in a range of cultured cells (44), the identity of the protease responsible for cleavage of CDCP1 in these lines has not been determined. This is in contrast with proteolytic processing of CDCP1

JBC

that occurs during metastasis *in vivo* which has recently been shown to be mediated in mice by plasmin (37). We propose that because not all cell lines that express 135 kDa CDCP1 also generate 70 kDa CDCP1 when grown in serum containing media (Fig 1A; OAW42 and SKOV-3 cells), either CDCP1 cleaving cell lines produce a protease that activates a latent protease present in serum that cleaves CDCP1, or these cell lines produce a protease that directly cleaves CDCP1. Based on comparison of the data for Caov3 and OVCA420 cells in Figure 1A (serum containing media) and 2B (serum free media +/- EGF), we suggest that EGF does not induce cleavage of CDCP1 via induction of either a protease that directly cleaves CDCP1 or a protease that activates a CDCP1 cleaving protease present in serum that has remained associated with the cells in serum free conditions. In addition, we also note from Figure 2B that there was no change in expression of the EMT markers E-cadherin (21) and N-cadherin (22) in response to EGF.

ERK signaling is required for EGF/EGFR-mediated upregulation of CDCP1–We also examined whether two known EGF/EGFR activated pathways are required for the observed increased expression of CDCP1. We first assessed whether these pathways (ERK (15, 16) and Src (8-13)) are activated downstream of EGF/EGFR in the two lines used in this study, Caov3 and OVCA420 cells. Western blot analysis showed that ERK (phosphorylation of T202/Y204) is rapidly activated in both cell lines in response to EGF and phosphorylation of this protein reduced gradually 8 to 24 h after initial stimulation (Fig 3A). In contrast, activation of Src (phosphorylation of Y416) paralleled the increases in CDCP1 expression seen in Figure 2B with increasing pSrc levels apparent after 0.5 h of EGF treatment and this was sustained up to 24 h (Fig 3A). In these experiments AG1478 treatment blocked phosphorylation of ERK and Src demonstrating that EGF-induced activation of these kinases was mediated by EGFR (Fig 3A). These data indicate that both ovarian cancer cell lines signal similarly in response to EGF/EGFR via ERK and Src.

Using selective pharmacological agents we examined if antagonism of these pathways affects EGF/EGFR-induced upregulation of CDCP1. Activation of ERK was inhibited with U0126 (48) and SFK activation with SU6656 (49). Inhibition of EGF/EGFR-induced expression of CDCP1 was quantified by densitometric analysis of Western blots of 3 independent experiments. This showed that the ~2 fold increase in CDCP1 expression induced by EGF in Caov3 and OVCA420 cells was reduced to background levels by U0126 inhibition of ERK (Fig 3B). In contrast, the SFK inhibitor SU6656 caused a 100% increase in CDCP1 expression above the effect of EGF in Caov3 cells and had no impact on its expression in OVCA420 cells (Fig 3B). EGF treatment in the presence of vehicle (0.1% DMSO) was used as positive control for upregulation of CDCP1 (Fig 3B). These data indicate that EGF/EGFR upregulation of CDCP1 requires signalling via the RAS/RAF/MEK/ERK pathway but not via SFKs.

EGF/EGFR signaling induces cell migration and relocalization of CDCP1–The effect of EGF/EGFR signaling on cell migration and localization of CDCP1 was examined by microscopy. As shown in Figure 4Aa-b, unstimulated and vehicle treated (0.1% DMSO) Caov3 cells grow as defined colonies. In response

JBC

to 24 h of EGF stimulation these cells acquire a spindle shaped morphology and migrate as evidenced by cell scattering (Fig 4Ac). Pre-treatment of Caov3 cells with the EGFR inhibitor AG1478 blocked both the transition to a spindle shaped morphology and cell scattering demonstrating that EGF-induced changes were mediated by EGFR (Fig 4Ad). OVCA420 cells, which grow as colonies that are less clearly defined than Caov3 cell colonies, also acquired a spindle shaped morphology and underwent cell scattering in response to EGF which was blocked by antagonism of EGFR (Fig 4Ae-h).

To examine the effect of EGF on the cellular localization of CDCP1, we performed confocal microscopy on unstimulated and EGF stimulated Caov3 and OVCA420 cells staining for CDCP1 (green), F-actin (red) and cell nuclei (blue). In unstimulated Caov3 and OVCA420 cells CDCP1 was largely restricted to the cell membrane at cell-cell contacts where it co-localized with F-actin (Fig 4Ba, b, e, f; yellow). However, 24 h after EGF treatment, intense punctuate CDCP1 staining was seen in the cytoplasm and also on the outside of the F-actin boundary of cells along filopodia that developed in response to EGF (Fig 4Bc, d, g, h; green). The relocalization of CDCP1 from cell-cell junctions to filopodia is consistent with this protein having a function in EGF-induced cell migration.

Disruption of CDCP1 expression and function reduces EGF-induced cell morphology changes and migration–Two approaches were employed to directly address the role of CDCP1 in EGF-induced cell migration. First, we interfered with the up-regulation of CDCP1 expression induced by EGF. Second, we disrupted CDCP1 function using a previously characterized monoclonal anti-CDCP1 antibody, 10D7, that blocks the ability of cancer cells to disseminate in chicken embryo and mouse models of metastasis (36, 37).

To interfere with EGF-induced upregulation of CDCP1, we generated polyclonal pools of Caov3 and OVCA420 cells stably infected with either a CDCP1 shRNA construct or a scramble control construct. The CDCP1 shRNA construct abolished CDCP1 expression in both Caov3 and OVCA420 cells compared to scramble controls and blocked the ability of EGF to induce, compared to the scramble control, upregulation of CDCP1 at both 0.2 and 24 h (Fig 5A). Microscopy analysis indicated that loss of CDCP1 had little impact on Caov3 and OVCA420 cell morphology (Fig 5B, -EGF, compare Scramble with shCDCP1). However, silencing of this protein reduced the ability of these cells to migrate and acquire an EGF-induced elongated spindle shaped morphology including the acquisition of filopodia (Fig 5B, +EGF, compare Scramble with shCDCP1). This qualitative analysis was confirmed by quantitative analysis of the distance between cells in 3 independent experiments which showed that silencing of CDCP1 blocked Caov3 and OCA420 cell migration induced by EGF (Fig 5C). These data suggest that the role of CDCP1 in EGF/EGFR-induced ovarian cancer cell morphological changes and increased migration requires its upregulation at the transcriptional level.

In experiments to assess the effect of blockade of CDCP1 function on EGF/EGFR-induced cell migration, Caov3 and OVCA420 cells in the presence and absence of the anti-CDCP1 antibody 10D7 were imaged by time-lapse microscopy,

JBC

collecting images every 15 min up to 12 h for OVCA420 cells and 24 h for Caov3 cells. Consistent with data in Figure 4A, images from time-lapse microscopy demonstrated that EGF treatment in the presence of control IgG induces a spindle shaped morphology and cell scattering in both cell lines (Fig 6A and B, IgG+EGF). These changes were inhibited by concomitant treatment with 10D7 consistent with a role for CDCP1 in EGF/EGFR-induced cell migration (Fig 6A and B). In Caov3 cells antibody blockade of cell morphological changes and migration was first apparent approximately 8 h after commencement of EGF treatment (Fig 6A, 10D7+EGF, 8 h). Quantitative analysis of at least 80 cells per treatment group showed that at 24 h EGF in the presence of IgG induced an increase of ~15 fold in migration over IgG only and this was decreased to an ~8 fold increase by 10D7 treatment (Fig 6A, graph). In OVCA420 cells blockade was first apparent about 4 h after commencement of EGF treatment (Fig 6B, 10D7+EGF, 4 h). Quantitative analysis of at least 80 cells per treatment group showed that at 12 h EGF treatment in the presence of IgG induced an increase of ~16 fold in migration over IgG only and this was decreased to an ~6 fold increase by 10D7 treatment (Fig 6B, graph). These data support a functional role for CDCP1 in the morphological changes and increased migration of ovarian cancer Caov3 and OVCA420 cells induced by EGF/EGFR.

CDCP1 is expressed by primary and metastatic ovarian tumors–To examine whether CDCP1 is expressed in ovarian cancer we performed immunohistochemical analysis on a series of ovarian cancers representing the progression from benign to malignant to metastatic disease including benign tumors from 3 patients, primary serous epithelial ovarian cancers from 3 patients and metastases from 3 patients. Representative images of anti-CDCP1 antibody and control staining are shown in Figure 7. Little expression of CDCP1 was seen in the 3 benign serous adenomas, while higher levels of CDCP1 staining was seen in primary (P) well differentiated (Grade 1) serous tumors (compare Fig 7A-B and 7C-D). The most intense CDCP1 staining was seen in the 3 metastatic (M) ovarian tumors (Fig 7E-G), including intense plasma membrane and cytoplasmic staining apparent in two of these metastases (Fig 7E-F). No staining was seen in control slides in which the primary antibody was replaced with rabbit IgG (Fig 7H). These data indicate that CDCP1 is expressed in epithelial ovarian tumors. A larger sample size is required to examine whether changes in expression of CDCP1 occur consistently during progression from adenoma to malignant ovarian cancer.

DISCUSSION

The EGF/EGFR axis has well studied roles in cell migration and cancer progression (25). Our data, which are summarized in Figure 8, define a new mechanism, involving the cell surface glycoprotein CDCP1, that regulates this cell migration signaling axis. We have demonstrated that disruption of CDCP1, either by silencing or the use of a function blocking antibody, substantially reduces the ability of EGF/EGFR to induce migration of ovarian cancer Caov3 and OVCA420 cells. Our data indicate that EGF/EGFR-induced cell migration is preceded by increased expression of CDCP1 and this increased expression is accompanied by relocalization of CDCP1 from cell-cell junctions to punctate structures on filopodia. Studies with pharmacological agents indicate that inhibition of

JBC

ERK but not Src signaling blocks upregulation of CDCP1 indicating that the RAS/RAF/MEK/ERK pathway is required downstream of EGF/EGFR to induce increased expression of CDCP1. Our observation from immunohistochemical analysis that CDCP1 is expressed by epithelial ovarian tumors has potential implications for treatment of this and other malignancies driven by EGF/EGFR signaling. In particular, it is possible that disruption of CDCP1 function may be a useful approach to limit the dissemination of cancer cells *in vivo*, including ovarian, lung and colorectal cancer cells, that are resistant to anti-EGFR therapies due to activating mutations in downstream signaling effectors such as RAS and RAF (25, 26, 50). It will be important to perform further analyses of larger patient cohorts to examine how CDCP1 expression alters with changes in expression and/or mutation of EGFR pathway components and whether targeting of CDCP1 represents a rational approach to treat these cancers.

EGF/EGFR regulation of CDCP1 is the third reported CDCP1 regulating pathway. The other pathways are: (i) SFK phosphorylation and (ii) hypoxia. SFK phosphorylation of CDCP1 is important for cancer cell survival, migration and invasion *in vitro* and *in vivo* (33, 34, 37, 51-53) and is activated in at least 3 cellular settings: cell de-adhesion, increased serine protease activity and overexpression of CDCP1 (45). Mechanistically it involves SFK phosphorylation of CDCP1 at tyrosine (Y) 734, Y734 and Y762, coupling of PKCδ at this last phospho-tyrosine and reciprocal activation of phosphorylation of SFKs at Y416 (34). Although we saw that pSrc-Y416 levels increased in parallel with the expression of CDCP1 induced by EGF/EGFR (compare Fig 3A and B with Fig 5A and B), we did not observe any change in phosphorylation of CDCP1-Y734 during EGF/EGFR-induced cell migration (data not shown). This indicates that mechanistically EGF/EGFR-mediated cell migration does not require phosphorylation of CDCP1 and suggests that in ovarian cancer cells, and potentially other cancer lines, signaling via EGF/EGFR and SFKs represent distinct CDCP1 regulating pathways.

In the second reported CDCP1 regulating pathway, expression of this protein is induced in kidney cancer cell lines by hypoxic conditions via a mechanism requiring the transcription factors HIF-1α and -2α (38). As EGFR is upstream of HIF signaling in prostate (54) and kidney (55) cancer cells it is possible that EGF/EGFR and HIF pathways may converge to regulate CDCP1 function. These reports on SFK and HIF regulation of CDCP1 and the current work are beginning to shed light on mechanisms controlling CDCP1 function and highlight the potential complexity of these pathways.

In our *in vitro* cell assays we were able to isolate EGF/EGFR regulated effects from other cellular modulators, such as proteolysis, by growing cells in serum free conditions. One of the interesting observations from these experiments was that there was no evidence of the 70 kDa CDCP1 species previously shown to be generated from the 135 kDa precursor protein by the *in vitro* action of serine proteases such as trypsin (31) and matriptase (32, 47) and *in vivo* by urokinase (31) and plasmin (39). However, in more complex cellular settings, such as serum containing *in vitro* cell culture and in animal models, EGF/EGFR regulation of CDCP1 will occur contemporaneously with other regulatory

JBC

mechanisms such as proteolysis and hypoxia. To understand how CDCP1 functions mechanistically to support EGF/EGFR-induced cell migration, we are currently exploring whether this pathway functions synergistically or in competition with serine protease and hypoxic regulation of CDCP1.

EGF via its receptor activates downstream signaling pathways that modify the cytoskeleton and initiate transcriptional and post-transcriptional regulation leading to altered cell plasticity and increased cell migration (56). We have shown that this signaling pathway not only initiates upregulation of CDCP1 mRNA and protein via activation of ERK, it also results in relocalization of CDCP1 from cell-cell junctions to punctate structures along filopodia. We propose that it is this repositioning of CDCP1 that is essential for its role in EGF/EGFR-induced cell migration. Our antibody-mediated blockade of CDCP1 prevented it from fulfilling this critical migration promoting role on filopdia. It is worth noting that although this antibody, 10D7, blocked ovarian cancer cell migration it had no impact on cell survival (not shown) in contrast with data from *in vivo* systems where this antibody caused apoptosis of cells escaping from blood vessels (36, 37). This would suggest that the ability of this antibody to induce cell death via blockade of CDCP1 function is context dependent. In *in vivo* settings where CDCP1 is promoting cell survival, antibody 10D7 blockade of this function induces cell death; however, *in vitro* this antibody blocks the role of CDCP1 in EGF/EGFR-induced cell migration without impacting on cell survival. This supports the proposal that the molecular mechanism regulating the role of CDCP1 in cell survival (SFK signaling) is distinct from the pathway promoting cell survival (EGF/EGFR signaling).

Interestingly, although EGF/EGFR signalling clearly altered the plasticity of ovarian cancer Caov3 and OVCA420 cells, resulting in loss of cell contact with neighbors, elongation and scattering (Fig 4), this was not accompanied by changes in expression of markers associated with an EMT (Fig 2B). This contrasts with two other ovarian cancer lines, OVCA433 and SKOV-3 cells, which undergo an EMT in response to EGF/EGFR activation as evidenced by changes in marker expression including decreased E-cadherin (21) and increased N-cadherin (22). EMT is thought to be required for the cell migration essential for a range of physiological processes as well as for progression of a number of cancers (57). However, the involvement of EMT in ovarian cancer is not clear because of the unique mixed epithelial and mesenchymal features of normal ovarian epithelium including low expression of the epithelial marker E-cadherin and expression of the mesenchymal markers keratin, vimentin and N-cadherin (17). In addition, analysis of patient samples indicates that in contrast with many other cancers, ovarian cancers express high levels of E-cadherin mRNA and protein (18, 58, 59). This lack of clarity on the role of EMT in ovarian cancer is also highlighted by cell line studies. For example, while some E-cadherin expressing ovarian cancer cells can be invasive *in vitro* and *in vivo* (60, 61), loss of expression of this protein promotes invasiveness of other ovarian cancer cell lines (62). Our data indicate that disruption of CDCP1 blocks the EGF/EGFR-induced migration of two ovarian cancer cell lines that do not show altered expression of EMT markers. It will be interesting to examine whether blockade of this protein can

JBC

also reduce the EGF/EGFR-induced migration of ovarian cancer cells that do undergo EMT.

In conclusion, these data highlight a novel role for the cell surface glycoprotein CDCP1 in EGF/EGFR-induced cell migration and indicate that targeting of CDCP1 may represent a rational approach to inhibit progression of cancers driven by this pathway.

REFERENCES

1. Ullrich, A., Coussens, L., Hayflick, J. S., Dull, T. J., Gray, A., Tam, A. W., Lee, J., Yarden, Y., Libermann, T. A., Schlessinger, J., and et al. (1984) *Nature* **309**, 418-425
2. Jorissen, R. N., Walker, F., Pouliot, N., Garrett, T. P., Ward, C. W., and Burgess, A. W. (2003) *Exp Cell Res* **284**, 31-53
3. Schneider, M. R., and Wolf, E. (2009) *J Cell Physiol* **218**, 460-466
4. Normanno, N., De Luca, A., Bianco, C., Strizzi, L., Mancino, M., Maiello, M. R., Carotenuto, A., De Feo, G., Caponigro, F., and Salomon, D. S. (2006) *Gene* **366**, 2-16
5. Downward, J., Waterfield, M. D., and Parker, P. J. (1985) *J Biol Chem* **260**, 14538-14546
6. Pierce, K. L., Tohgo, A., Ahn, S., Field, M. E., Luttrell, L. M., and Lefkowitz, R. J. (2001) *J Biol Chem* **276**, 23155-23160
7. Poon, S. L., Hammond, G. T., and Leung, P. C. (2009) *Mol Endocrinol* **23**, 1646-1656
8. Mao, W., Irby, R., Coppola, D., Fu, L., Wloch, M., Turner, J., Yu, H., Garcia, R., Jove, R., and Yeatman, T. J. (1997) *Oncogene* **15**, 3083-3090
9. Ricono, J. M., Huang, M., Barnes, L. A., Lau, S. K., Weis, S. M., Schlaepfer, D. D., Hanks, S. K., and Cheresh, D. A. (2009) *Cancer Res* **69**, 1383-1391
10. Yarden, Y., and Sliwkowski, M. X. (2001) *Nat Rev Mol Cell Biol* **2**, 127-137
11. Kim, L. C., Song, L., and Haura, E. B. (2009) *Nat Rev Clin Oncol* **6**, 587-595
12. Chung, B. M., Dimri, M., George, M., Reddi, A. L., Chen, G., Band, V., and Band, H. (2009) *Oncogene* **28**, 1821-1832
13. Maa, M. C., Leu, T. H., McCarley, D. J., Schatzman, R. C., and Parsons, S. J. (1995) *Proc Natl Acad Sci U S A* **92**, 6981-6985
14. Wells, A. (1999) *Int J Biochem Cell Biol* **31**, 637-643
15. Sibilia, M., Fleischmann, A., Behrens, A., Stingl, L., Carroll, J., Watt, F. M., Schlessinger, J., and Wagner, E. F. (2000) *Cell* **102**, 211-220
16. Shilo, B. Z. (2003) *Exp Cell Res* **284**, 140-149
17. Ahmed, N., Thompson, E. W., and Quinn, M. A. (2007) *J Cell Physiol* **213**, 581-588
18. Hudson, L. G., Zeineldin, R., and Stack, M. S. (2008) *Clin Exp Metastasis* **25**, 643-655
19. Zeineldin, R., Muller, C. Y., Stack, M. S., and Hudson, L. G. (2010) *J Oncol*, 414676
20. Lu, Z., Ghosh, S., Wang, Z., and Hunter, T. (2003) *Cancer Cell* **4**, 499-515
21. Lim, R., Ahmed, N., Borregaard, N., Riley, C., Wafai, R., Thompson, E. W., Quinn, M. A., and Rice, G. E. (2007) *Int J Cancer* **120**, 2426-2434

JBC

22. Colomiere, M., Ward, A. C., Riley, C., Trenerry, M. K., Cameron-Smith, D., Findlay, J., Ackland, L., and Ahmed, N. (2009) *Br J Cancer* **100**, 134-144
23. Lee, M. Y., Chou, C. Y., Tang, M. J., and Shen, M. R. (2008) *Clin Cancer Res* **14**, 4743-4750
24. Prenzel, N., Fischer, O. M., Streit, S., Hart, S., and Ullrich, A. (2001) *Endocr Relat Cancer* **8**, 11-31
25. Wheeler, D. L., Dunn, E. F., and Harari, P. M. (2010) *Nat Rev Clin Oncol* **7**, 493-507
26. Gotoh, N. (2011) *Int J Clin Exp Pathol* **4**, 403-409
27. Scherl-Mostageer, M., Sommergruber, W., Abseher, R., Hauptmann, R., Ambros, P., and Schweifer, N. (2001) *Oncogene* **20**, 4402-4408
28. Hooper, J. D., Zijlstra, A., Aimes, R. T., Liang, H., Claassen, G. F., Tarin, D., Testa, J. E., and Quigley, J. P. (2003) *Oncogene* **22**, 1783-1794
29. Brown, T. A., Yang, T. M., Zaitsevskaia, T., Xia, Y., Dunn, C. A., Sigle, R. O., Knudsen, B., and Carter, W. G. (2004) *J Biol Chem* **279**, 14772-14783
30. Bhatt, A. S., Erdjument-Bromage, H., Tempst, P., Craik, C. S., and Moasser, M. M. (2005) *Oncogene* **24**, 5333-5343
31. Uekita, T., and Sakai, R. (2011) *Cancer Sci* **102**, 1943-1948
32. Wortmann, A., He, Y., Deryugina, E. I., Quigley, J. P., and Hooper, J. D. (2009) *IUBMB Life* **61**, 723-730
33. Uekita, T., Tanaka, M., Takigahira, M., Miyazawa, Y., Nakanishi, Y., Kanai, Y., Yanagihara, K., and Sakai, R. (2008) *Am J Pathol* **172**, 1729-1739
34. Miyazawa, Y., Uekita, T., Hiraoka, N., Fujii, S., Kosuge, T., Kanai, Y., Nojima, Y., and Sakai, R. (2010) *Cancer Res* **70**, 5136-5146
35. Siva, A. C., Wild, M. A., Kirkland, R. E., Nolan, M. J., Lin, B., Maruyama, T., Yantiri-Wernimont, F., Frederickson, S., Bowdish, K. S., and Xin, H. (2008) *Cancer Res* **68**, 3759-3766
36. Deryugina, E. I., Conn, E. M., Wortmann, A., Partridge, J. J., Kupriyanova, T. A., Ardi, V. C., Hooper, J. D., and Quigley, J. P. (2009) *Mol Cancer Res* **7**, 1197-1211
37. Casar, B., He, Y., Iconomou, M., Hooper, J. D., Quigley, J. P., and Deryugina, E. I. (2011) *Oncogene* **In press**
38. Razorenova, O. V., Finger, E. C., Colavitti, R., Chernikova, S. B., Boiko, A. D., Chan, C. K., Krieg, A., Bedogni, B., LaGory, E., Weissman, I. L., Broome-Powell, M., and Giaccia, A. J. (2011) *Proc Natl Acad Sci U S A* **108**, 1931-1936
39. Deryugina, E. I., Conn, E. M., Wortmann, A., Partridge, J. J., Kupriyanova, T. A., Ardi, V. C., Hooper, J. D., and Quigley, J. P. (2009) *Molecular Cancer Research* **7**, 1197-1211
40. Dong, Y., Kaushal, A., Bui, L., Chu, S., Fuller, P. J., Nicklin, J., Samaratunga, H., and Clements, J. A. (2001) *Clin Cancer Res* **7**, 2363-2371
41. Tsao, S. W., Mok, S. C., Fey, E. G., Fletcher, J. A., Wan, T. S., Chew, E. C., Muto, M. G., Knapp, R. C., and Berkowitz, R. S. (1995) *Exp Cell Res* **218**, 499-507
42. Fischer, K., Lutz, V., Wilhelm, O., Schmitt, M., Graeff, H., Heiss, P., Nishiguchi, T., Harbeck, N., Kessler, H., Luther, T., Magdolen, V., and Reuning, U. (1998) *FEBS Lett* **438**, 101-105.

JBC

43. Dong, Y., Tan, O. L., Loessner, D., Stephens, C., Walpole, C., Boyle, G. M., Parsons, P. G., and Clements, J. A. (2010) *Cancer Res* **70**, 2624-2633
44. He, Y., Wortmann, A., Burke, L. J., Reid, J. C., Adams, M. N., Abdul-Jabbar, I., Quigley, J. P., Leduc, R., Kirchhofer, D., and Hooper, J. D. (2010) *J Biol Chem* **285**, 26162-26173
45. Wortmann, A., He, Y., Christensen, M. E., Linn, M., Lumley, J. W., Pollock, P. M., Waterhouse, N. J., and Hooper, J. D. (2011) *J Biol Chem* **286**, 42303-42315
46. Yamauchi, T., Ueki, K., Tobe, K., Tamemoto, H., Sekine, N., Wada, M., Honjo, M., Takahashi, M., Takahashi, T., Hirai, H., Tushima, T., Akanuma, Y., Fujita, T., Komuro, I., Yazaki, Y., and Kadowaki, T. (1997) *Nature* **390**, 91-96
47. Levitzki, A., and Gazit, A. (1995) *Science* **267**, 1782-1788
48. MacKeigan, J. P., Collins, T. S., and Ting, J. P. (2000) *J Biol Chem* **275**, 38953-38956
49. Blake, R. A., Broome, M. A., Liu, X., Wu, J., Gishizky, M., Sun, L., and Courtneidge, S. A. (2000) *Mol Cell Biol* **20**, 9018-9027
50. Ciardiello, F., and Tortora, G. (2008) *N Engl J Med* **358**, 1160-1174
51. Uekita, T., Jia, L., Narisawa-Saito, M., Yokota, J., Kiyono, T., and Sakai, R. (2007) *Mol Cell Biol* **27**, 7649-7660
52. Liu, H., Ong, S. E., Badu-Nkansah, K., Schindler, J., White, F. M., and Hynes, R. O. (2011) *Proc Natl Acad Sci U S A* **108**, 1379-1384
53. Benes, C. H., Poulogiannis, G., Cantley, L. C., and Soltoff, S. P. (2011) *Oncogene* **In press**
54. Zhong, H., Chiles, K., Feldser, D., Laughner, E., Hanrahan, C., Georgescu, M. M., Simons, J. W., and Semenza, G. L. (2000) *Cancer Res* **60**, 1541-1545
55. Smith, K., Gunaratnam, L., Morley, M., Franovic, A., Mekhail, K., and Lee, S. (2005) *Cancer Res* **65**, 5221-5230
56. Oda, K., Matsuoka, Y., Funahashi, A., and Kitano, H. (2005) *Mol Syst Biol* **1**, 2005 0010
57. Thiery, J. P. (2002) *Nat Rev Cancer* **2**, 442-454
58. Santin, A. D., Zhan, F., Bellone, S., Palmieri, M., Cane, S., Bignotti, E., Anfossi, S., Gokden, M., Dunn, D., Roman, J. J., O'Brien, T. J., Tian, E., Cannon, M. J., Shaughnessy, J., Jr., and Pecorelli, S. (2004) *Int J Cancer* **112**, 14-25
59. Bendoraite, A., Knouf, E. C., Garg, K. S., Parkin, R. K., Kroh, E. M., O'Briant, K. C., Ventura, A. P., Godwin, A. K., Karlan, B. Y., Drescher, C. W., Urban, N., Knudsen, B. S., and Tewari, M. (2010) *Gynecol Oncol* **116**, 117-125
60. Strauss, R., Li, Z. Y., Liu, Y., Beyer, I., Persson, J., Sova, P., Moller, T., Pesonen, S., Hemminki, A., Hamerlik, P., Drescher, C., Urban, N., Bartek, J., and Lieber, A. (2011) *PLoS One* **6**, e16186
61. Ong, A., Maines-Bandiera, S. L., Roskelley, C. D., and Auersperg, N. (2000) *Int J Cancer* **85**, 430-437
62. Cowden Dahl, K. D., Symowicz, J., Ning, Y., Gutierrez, E., Fishman, D. A., Adley, B. P., Stack, M. S., and Hudson, L. G. (2008) *Cancer Res* **68**, 4606-4613

JBC

FOOTNOTES

The abbreviations used are: CDCP1, CUB-domain containing protein 1; DAPI, 4'-6-Diamidino-2-phenylindole; EDTA, ethylene diamin tetra-acetic acid; FCS, fetal calf serum; GAPDH, glyceraldehyde-3-phosphate dehydrogenase; IgG, immunoglobulin; SFK, Src family kinase.

ACKNOWLEDGEMENTS

We thank Dr Lez Burke for culture of hybridomas and purification of immunoglobulins, Professor Samuel Mok (University of Texas MD Anderson Cancer Center) for the kind gift of OVCA420 cells and Professor Viktor Magdolen for the kind gift of OVMZ-6 cells. This work was funded by the Wesley Research Institute (grant #2008/06 to JDH), the Cancer Council Queensland (grant #614205 to JDH) and the National Health and Medical Research Council of Australia (NHMRC grant #550523 to YD and JAC; Principal Research Fellowship #1005717 to JAC).

FIGURE LEGENDS

FIGURE 1. **CDCP1 expression in ovarian cancer cell lines.** *A,* Anti-CDCP1 and anti-GAPDH Western blot analysis of lysates from 10 ovarian cancer cell lines and normal foreskin fibroblasts (NFF) cultured in media containing 10% serum. The molecular weight of the CDCP1 bands at 70 and 135 kDa are indicated. *B,* Anti-pEGFR (Y1068) and anti-GAPDH Western blot analysis of lysates from Caov3, OVCA420, OVCA432 and PEO4 ovarian cancer cell lines cultured in serum free media either untreated or EGF treated (30 ng/ml in 0.1% DMSO) for the indicated times.

FIGURE 2. **CDCP1 is upregulated by EGF activation of EGFR.** *A,* Graphical representation of fold change in *CDCP1* mRNA levels relative to *HPRT1* mRNA in response to EGF (30 ng/ml) in serum free media at 0.2 and 24 h. Bars represent fold change assessed using the ΔC_T method. Data are mean ± SEM from 3 separate experiments with triplicate wells per experiment. *B,* Anti-CDCP1, -E-cadherin, -N-cadherin and -GAPDH Western blot analysis of lysates from Caov3 cells. *C,* Anti-CDCP1, -E-cadherin, -N-cadherin and -GAPDH Western blot analysis of lysates from OVCA420 cells. In *B* and *C* lysates were from cells grown in serum free media (lane 1), 0.1% DMSO (lane 2); 0.1% DMSO and EGF (30 ng/ml) for 0.1, 0.2, 0.5, 1, 8 and 24 h (lane 3-8); 0.1% DMSO, EGF (30 ng/ml) and AG1478 (20 μM) for 0.2 and 24 h (lane 9-10). Graphical representation of densitometry analysis of anti-CDCP1 Western blot data from 3 independent experiments is shown below each panel. The ratio of the signal intensity of 135 kDa CDCP to GAPDH at each time point was normalized to the DMSO control.

FIGURE 3. **ERK signaling is required for EGF/EGFR mediated upregulation of CDCP1.** *A,* Western blot analysis of pSrc-Y416 and Src, pERK1/2-Y202/204 and ERK1/2, pEGFR-Y1068 and EGFR in Caov3 (left) and OVCA420 (right) ovarian cancer cells. GAPDH was used as a loading control. Cells were grown in serum free culture media (lane 1), 0.1% DMSO (lane 2); 0.1% DMSO and EGF (30 ng/ml) for 0.1, 0.2, 0.5, 1, 8 and 24 h (lane 3-8); 0.1% DMSO, EGF (30 ng/ml) and AG1478 (20 μM) for 0.2 and 24 h (lane 9-10). These data are representative of 3 independent experiments. *B,* Graphical representation

JBC

of densitometry analysis of 3 independent anti-CDCP1 Western blot analyses. Caov3 and OVCA420 cells were treated for 0.2 and 24 h with 0.1% DMSO; EGF (30 ng/ml) and 0.1% DMSO; EGF (30 ng/ml), 0.1% DMSO and SU6656 (10 μM); or EGF (30 ng/ml), 0.1% DMSO and U0126 (10 μM). Values were obtained from the intensity of the 135 kDa CDCP1 band, normalized to GAPDH, relative to the untreated control. Statistical significance was examined using a Student's t-test; * $p < 0.05$.

FIGURE 4. **Relocalization of CDCP1 during EGF/EGFR-induced cell migration.** *A,* Phase contrast microscopy showing morphology of Caov3 and OVCA420 cells grown in serum free media and either untreated (a, e), or treated with 0.1% DMSO (b, f), 0.1% DMSO with EGF (30 ng/ml) (c, g) or 0.1% DMSO with EGF (30 ng/ml) and AG1478 (20 μM) (d, h) for 24 h. Data are representative of at least 3 independent experiments. Bar, 100 μm. *B,* Confocal microscopy analysis of Caov3 and OVCA420 cells either untreated (a, b, e, f) or treated with 0.1% DMSO with EGF (30 ng/ml) (c, d, g, h) for 24 h. Cells were stained with anti-CDCP1 antibody 10D7 followed by a fluorescently labeled anti-mouse secondary antibody (green), AlexaFluor 568 phalloidin to stain F-actin (red) and DAPI to stain cell nuclei (blue). Scale bars are as indicated.

FIGURE 5. **Upregulation of CDCP1 mRNA is required for EGF-induced cell migration.** *A,* Western blot analysis of CDCP1 and GAPDH expression in Caov3 and OVCA420 cells stably transfected with either a scramble control (Scramble) or CDCP1 pLKO.1 lentiviral shRNA (shCDCP1). Cells were either untreated (-) or treated with EGF (30 ng/ml in 0.1% DMSO) for 0.2 and 24 h in serum free media. *B,* Representative phase contrast microscopy images of scramble and shCDCP1 Caov3 and OVCA420 cells +/- EGF (30 ng/ml in 0.1% DMSO) for 24 h. *C,* Graphical representation of the effect of CDCP1 silencing on cell migration induced by EGF. Migration at 2 and 24 h was assessed as the distance between cell nuclei in 3 independent experiments using InDesign software (Adobe, Adobe Systems Pty Ltd, Chatswood, Australia). Measurements were performed on 200 pairs of cells from 10 randomly selected fields per treatment group. Statistical significance was examined using a Student's t-test; * $p < 0.05$, ** $p < 0.01$, *** $p < 0.001$. Scale bar, 50 μm.

FIGURE 6. **Antibody blockade of CDCP1 reduces EGF-induced cell morphology changes and increased migration** Representative time lapse phase contrast microscopy images showing morphology and scattering of cells treated with either mouse IgG (20 μg/ml) as a control, EGF (30 ng/ml) and mouse IgG, or EGF (30 ng/ml) and CDCP1 function blocking antibody 10D7 (20 μg/ml) in serum free media. *A,* Caov3 cells. Representative images from 0, 8, 16 and 24 h are shown. *B,* OVCA420 cells. Representative images from 0, 4, 8 and 12 h are shown. On the right of each panel is the graphical representation of accumulated migration distance at 24 h for Caov3 cells and at 12 h for OVCA420 cells. The distance between cell nuclei was determined for at least 80 randomly selected cells for each treatment using MetaMorph Software Version 7.0.3 (Molecular Devices, Bio-Strategy, Hawthorne East, Australia). Statistical significance was evaluated using a Student's t-test. *, $p < 0.05$; **, $p < 0.01$. Scale bar, 50 μm.

JBC

FIGURE 7. **CDCP1 is expressed during progression of epithelial ovarian cancer.** Tissue sections from 3 benign serous ovarian adenomas, 3 primary serous epithelial ovarian cancers and 3 ovarian cancer metastases were stained with a rabbit anti-CDCP1 antibody or control rabbit IgG followed by a horse-radish peroxidase conjugated secondary antibody. Positive CDCP1 signal appears as brown coloration. Representative images are shown. *A-B,* Benign serous adenoma. *C-D,* Well differentiated serous epithelial ovarian cancer from a primary (P) tumor. *E-G,* Poorly differentiated serous epithelial ovarian cancer metastases (M) to the omentum. *H,* Negative control where rabbit IgG replaced the primary antibody. Tumor grade is indicated above the relevant panel. Scale bar, 50 μm.

FIGURE 8. **Schematic representation of pathways required for the role of CDCP1 in EGF/EGFR-induced cell morphological changes and increased cell migration.** CDCP1 mediates, at least in part, EGF/EGFR-induced cell morphological changes and increased migration. EGF signals via EGFR (as indicated through use of the EGFR antagonist AG1478) to induce signaling via ERK that leads to upregulation of CDCP1 mRNA and protein. Targeting of CDCP1, either via silencing of its mRNA or through use of an anti-CDCP1 function blocking antibody, is effective at reducing these EGF-induced effects. Approaches that disrupt CDCP1 function may be useful to inhibit progression of malignancies driven by EGFR signaling, such as ovarian cancer, and those resistant to anti-EGFR drugs because of activating mutations in the RAS/RAF/MEK/ERK pathway.

JBC

Fig 1

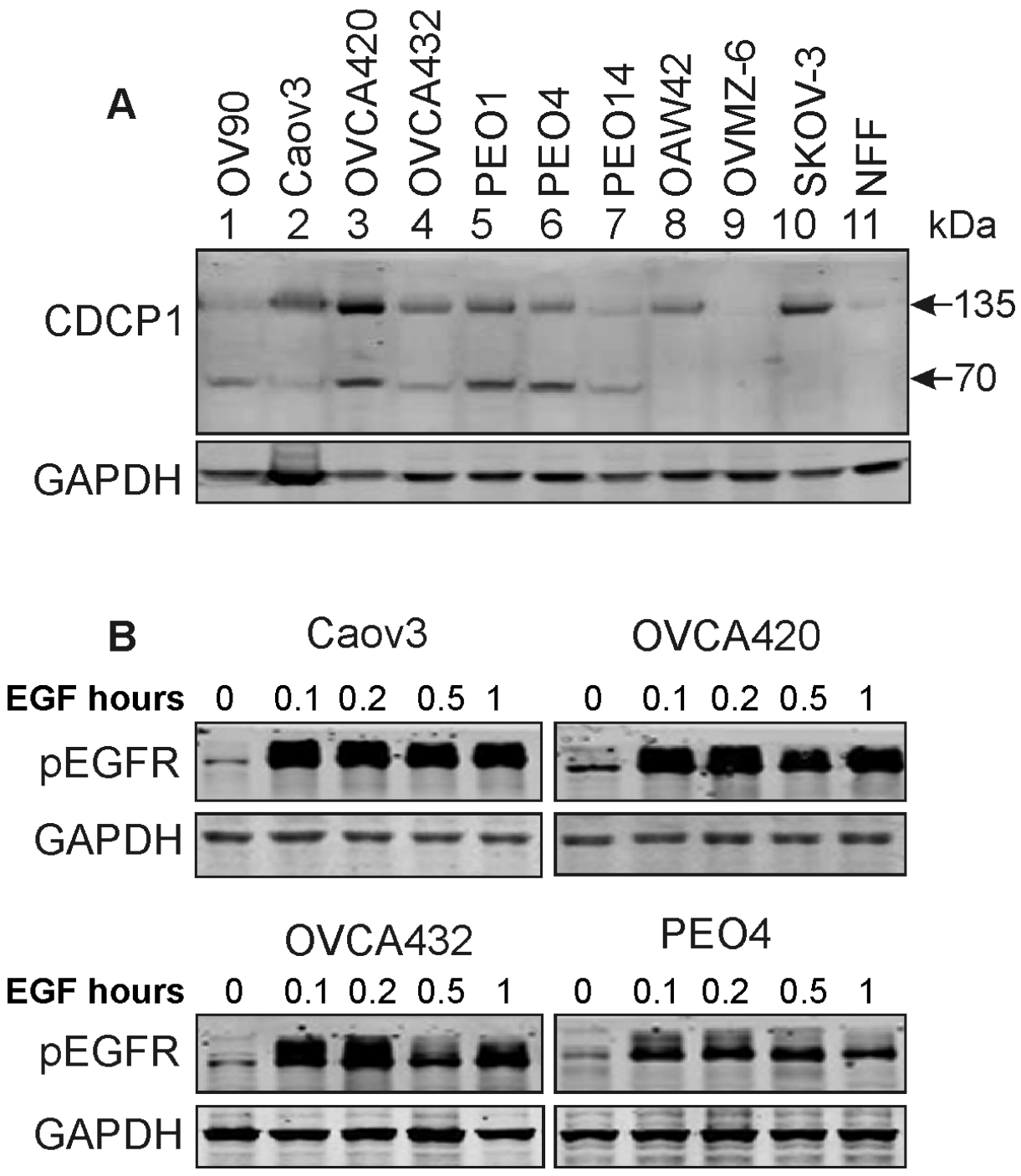
A
OV90
Caov3
OVCA420
OVCA432
PEO1
PEO4
PEO14
OAW42
OVMZ-6
SKOV-3
NFF
1 2 3 4 5 6 7 8 9 10 11
kDa
CDCP1
135
70
GAPDH
B
Caov3
OVCA420
EGF hours 0 0.1 0.2 0.5 1
pEGFR
GAPDH
OVCA432
PEO4
EGF hours 0 0.1 0.2 0.5 1
pEGFR
GAPDH

JBC

Fig 2

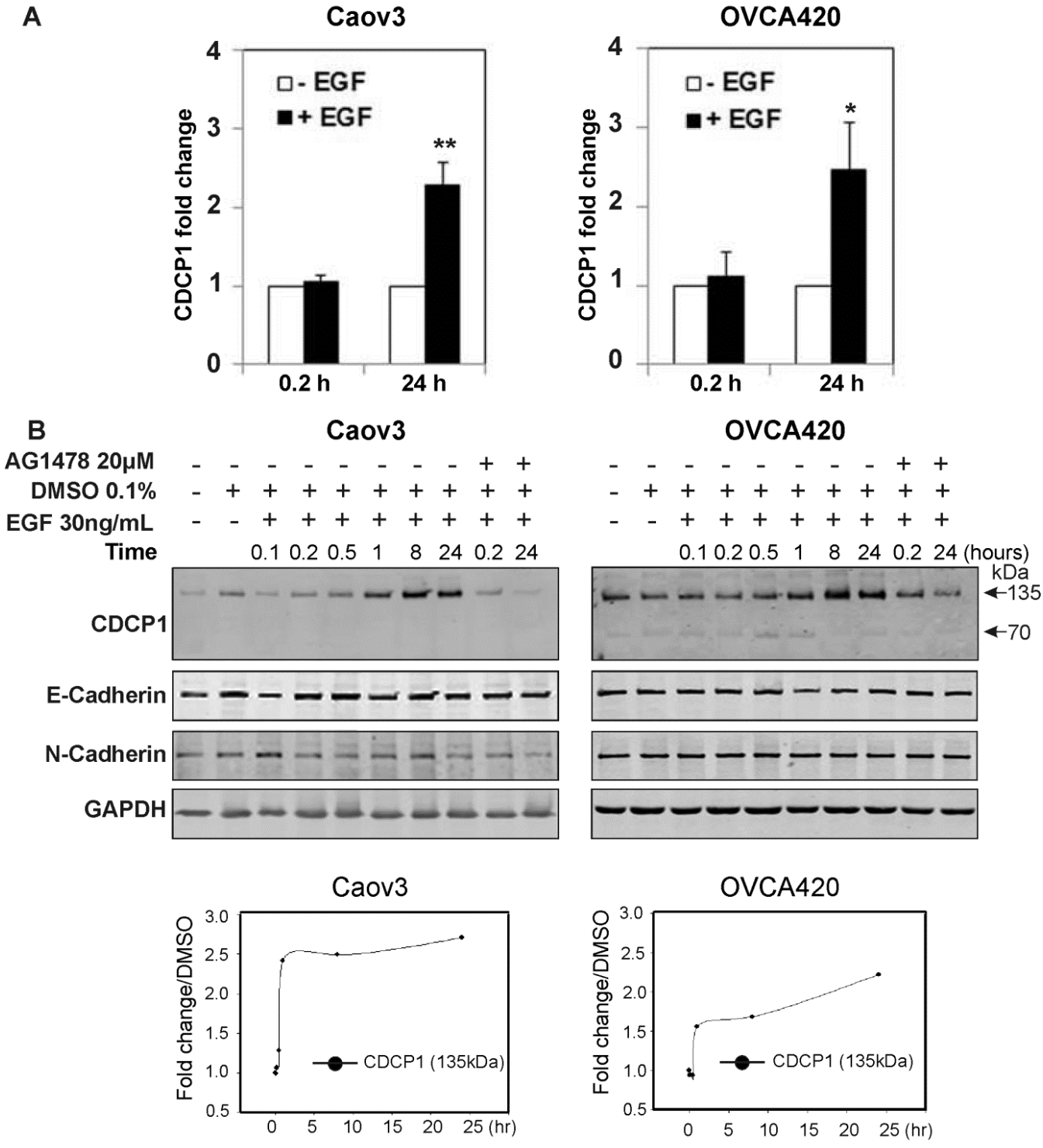
A
Caov3
OVCA420
- EGF
+ EGF
CDCP1 fold change
0.2 h
24 h
**
*
B
AG1478 20μM
DMSO 0.1%
EGF 30ng/mL
Time
0.1 0.2 0.5 1 8 24 0.2 24 (hours)
kDa
135
70
CDCP1
E-Cadherin
N-Cadherin
GAPDH
Fold change/DMSO
CDCP1 (135kDa)
25 (hr)

JBC

Fig 3

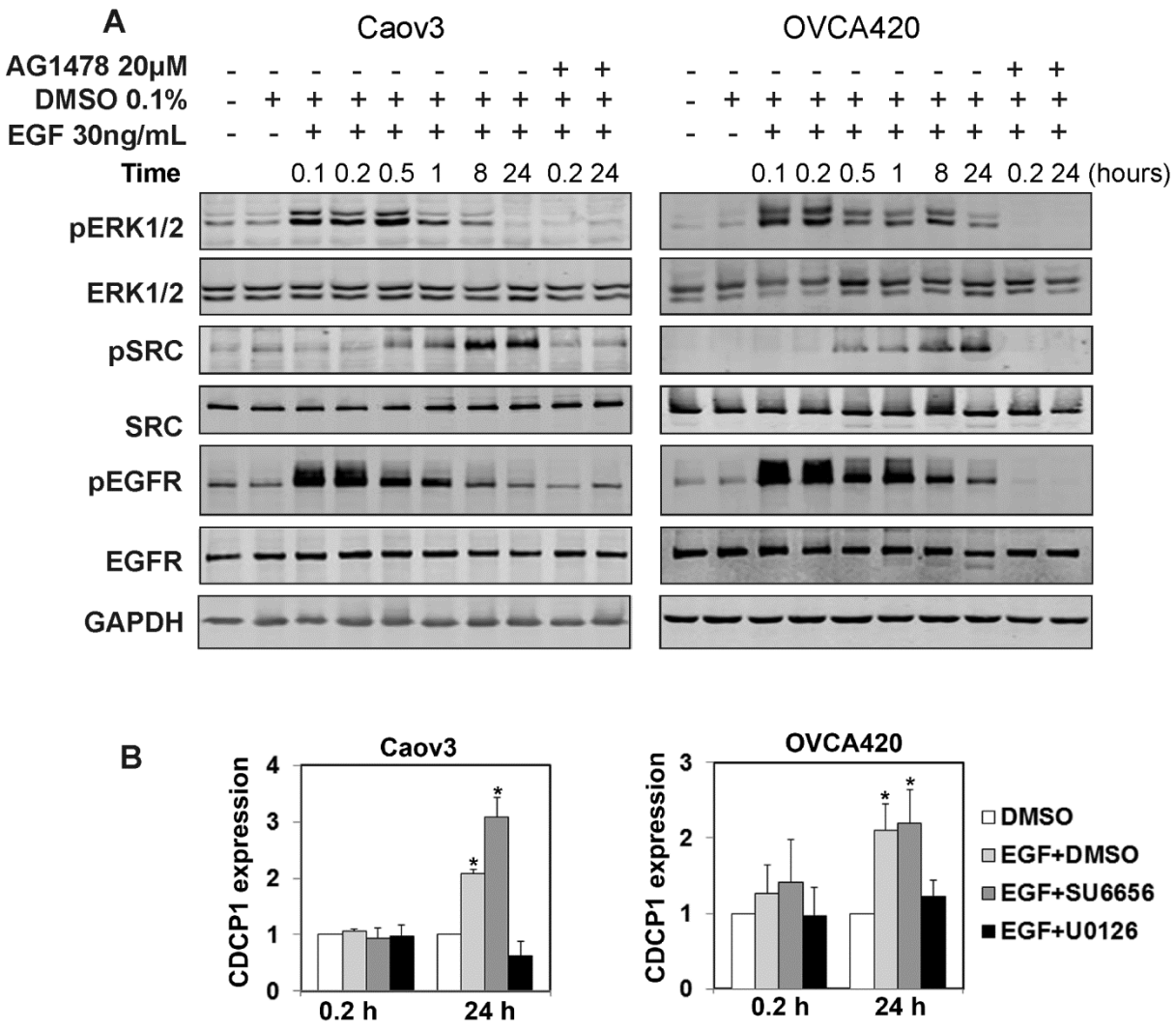
A
Caov3
OVCA420
AG1478 20μM
DMSO 0.1%
EGF 30ng/mL
Time
0.1 0.2 0.5 1 8 24 0.2 24
0.1 0.2 0.5 1 8 24 0.2 24 (hours)
pERK1/2
ERK1/2
pSRC
SRC
pEGFR
EGFR
GAPDH
B
Caov3
OVCA420
CDCP1 expression
0.2 h
24 h
DMSO
EGF+DMSO
EGF+SU6656
EGF+U0126

JBC

Fig 4

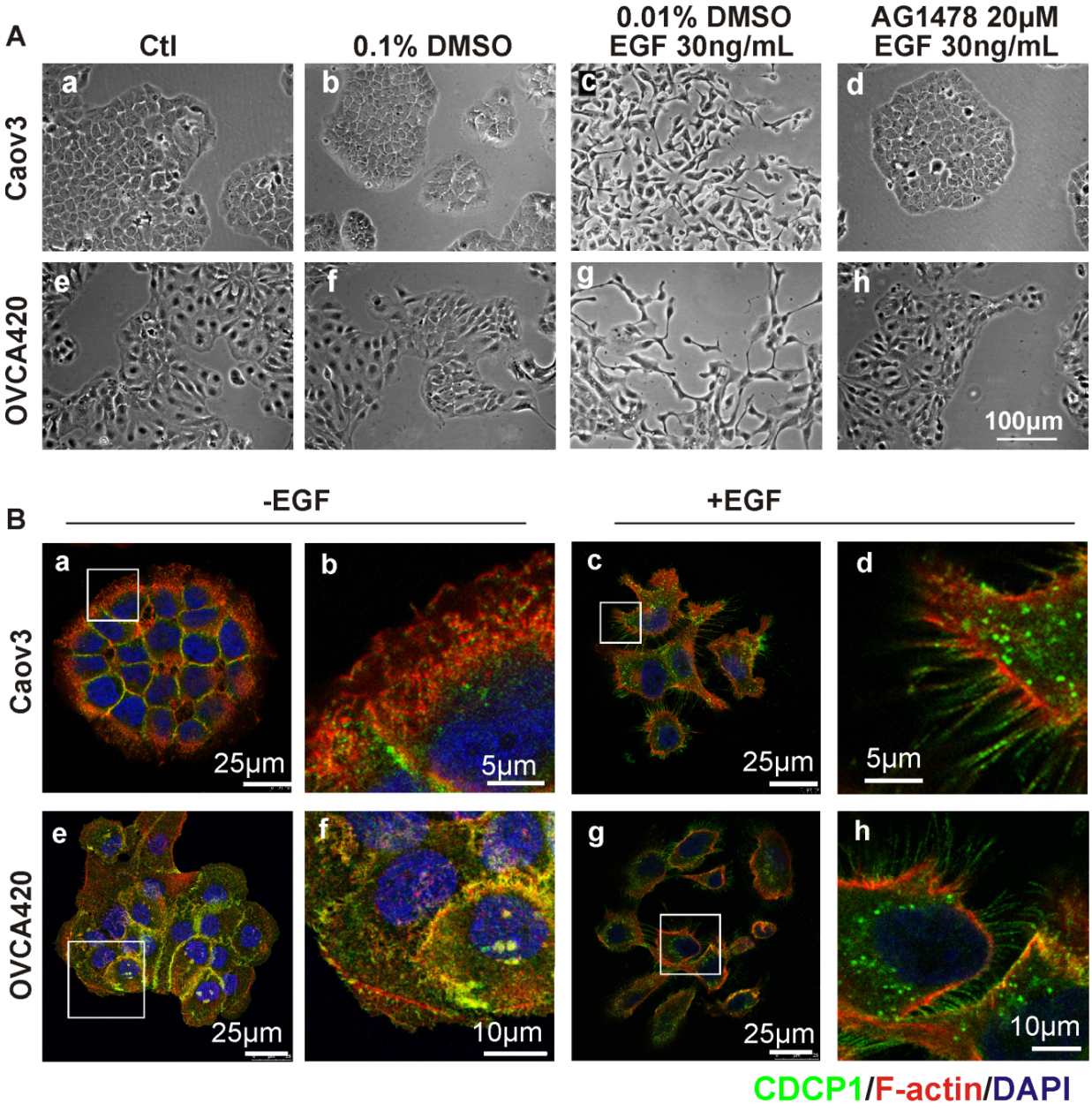
A
Ctl
0.1% DMSO
0.01% DMSO
EGF 30ng/mL
AG1478 20μM
EGF 30ng/mL
Caov3
OVCA420
a
b
c
d
e
f
g
h
100μm
B
-EGF
+EGF
Caov3
OVCA420
25μm
5μm
25μm
5μm
25μm
10μm
25μm
10μm
CDCP1/F-actin/DAPI

JBC

Fig 5

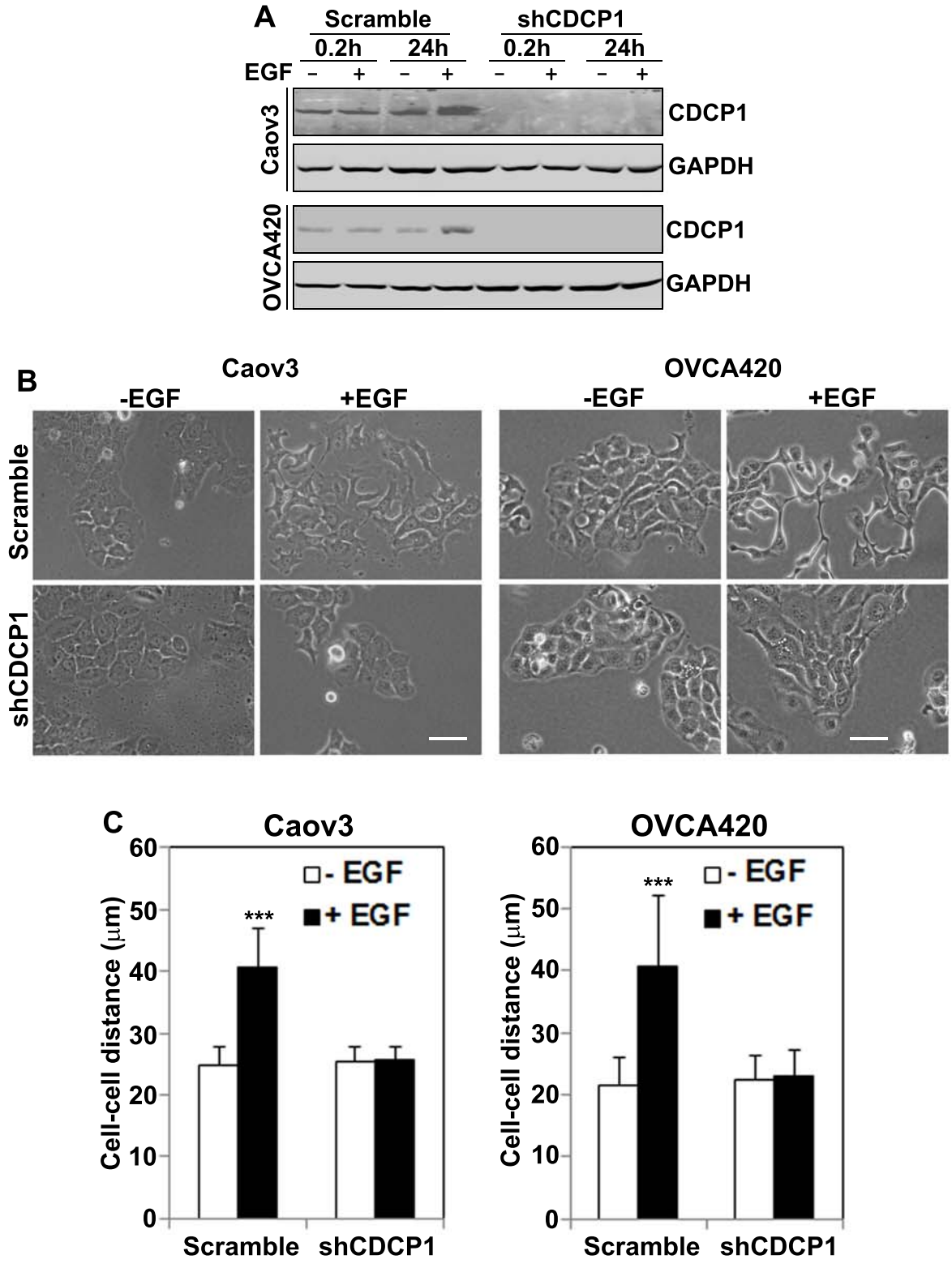
A
Scramble
shCDCP1
0.2h
24h
0.2h
24h
EGF
– + – + – + – +
Caov3
CDCP1
GAPDH
OVCA420
CDCP1
GAPDH
B
Caov3
OVCA420
-EGF
+EGF
-EGF
+EGF
Scramble
shCDCP1
C
Caov3
OVCA420
Cell-cell distance (μm)
0
10
20
30
40
50
60
***
- EGF
+ EGF
Scramble
shCDCP1

JBC

Fig 6

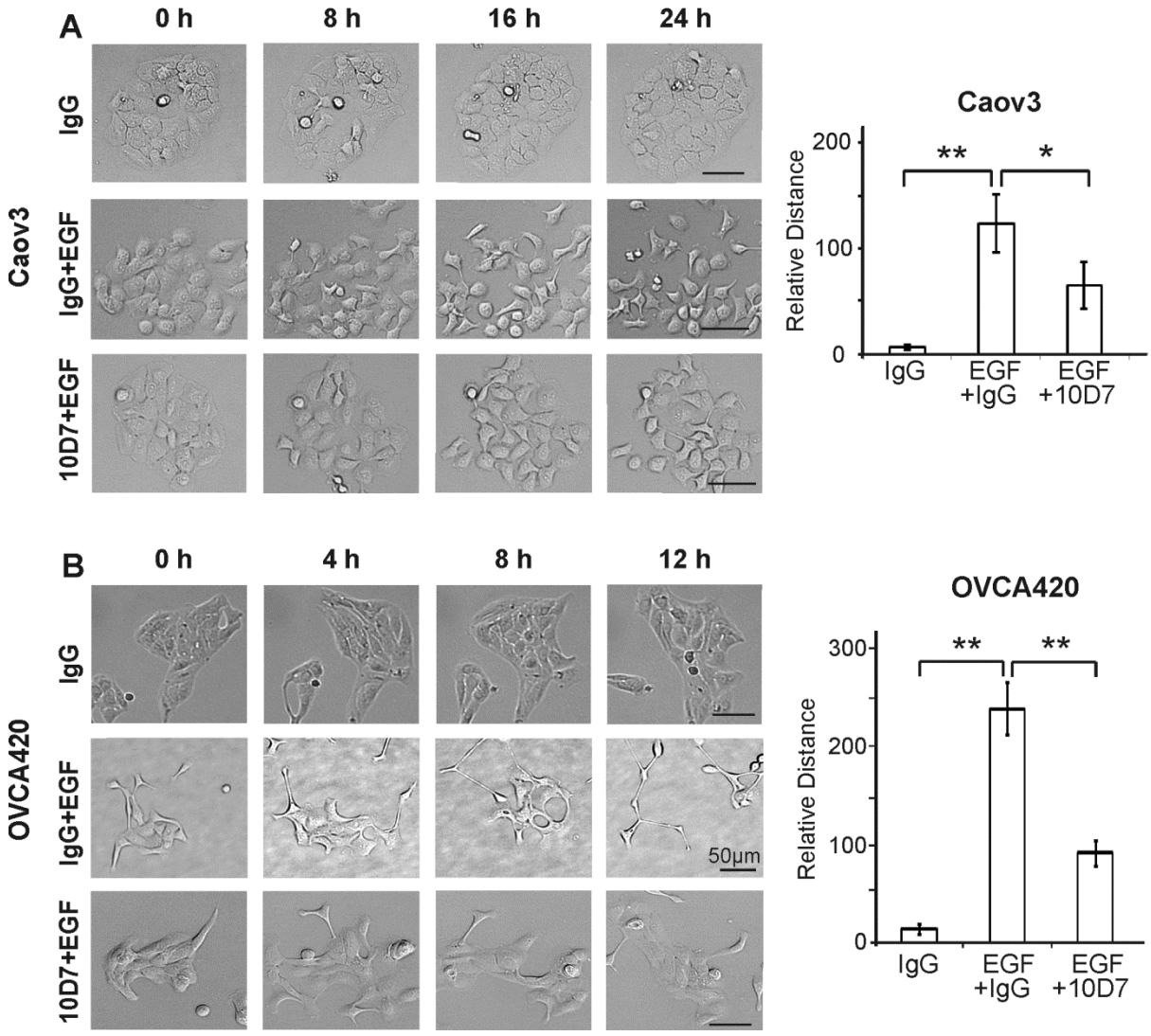
A
0 h
8 h
16 h
24 h
IgG
IgG+EGF
10D7+EGF
Caov3
Caov3
Relative Distance
200
100
0
**
*
IgG
EGF +IgG
EGF +10D7
B
0 h
4 h
8 h
12 h
IgG
IgG+EGF
10D7+EGF
OVCA420
50μm
OVCA420
Relative Distance
300
200
100
0
**
**
IgG
EGF +IgG
EGF +10D7

JBC

Fig 7

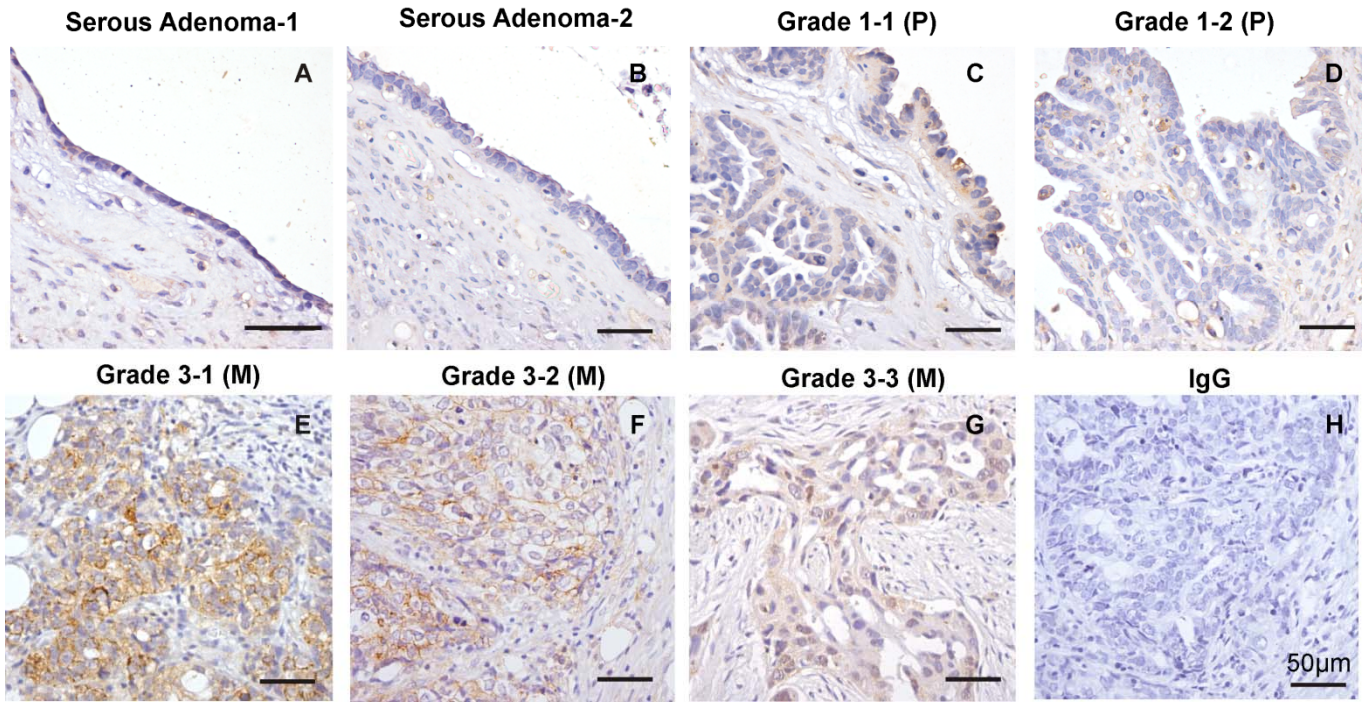
Serous Adenoma-1
Serous Adenoma-2
Grade 1-1 (P)
Grade 1-2 (P)
A
B
C
D
Grade 3-1 (M)
Grade 3-2 (M)
Grade 3-3 (M)
IgG
E
F
G
H
50μm

JBC

Fig 8

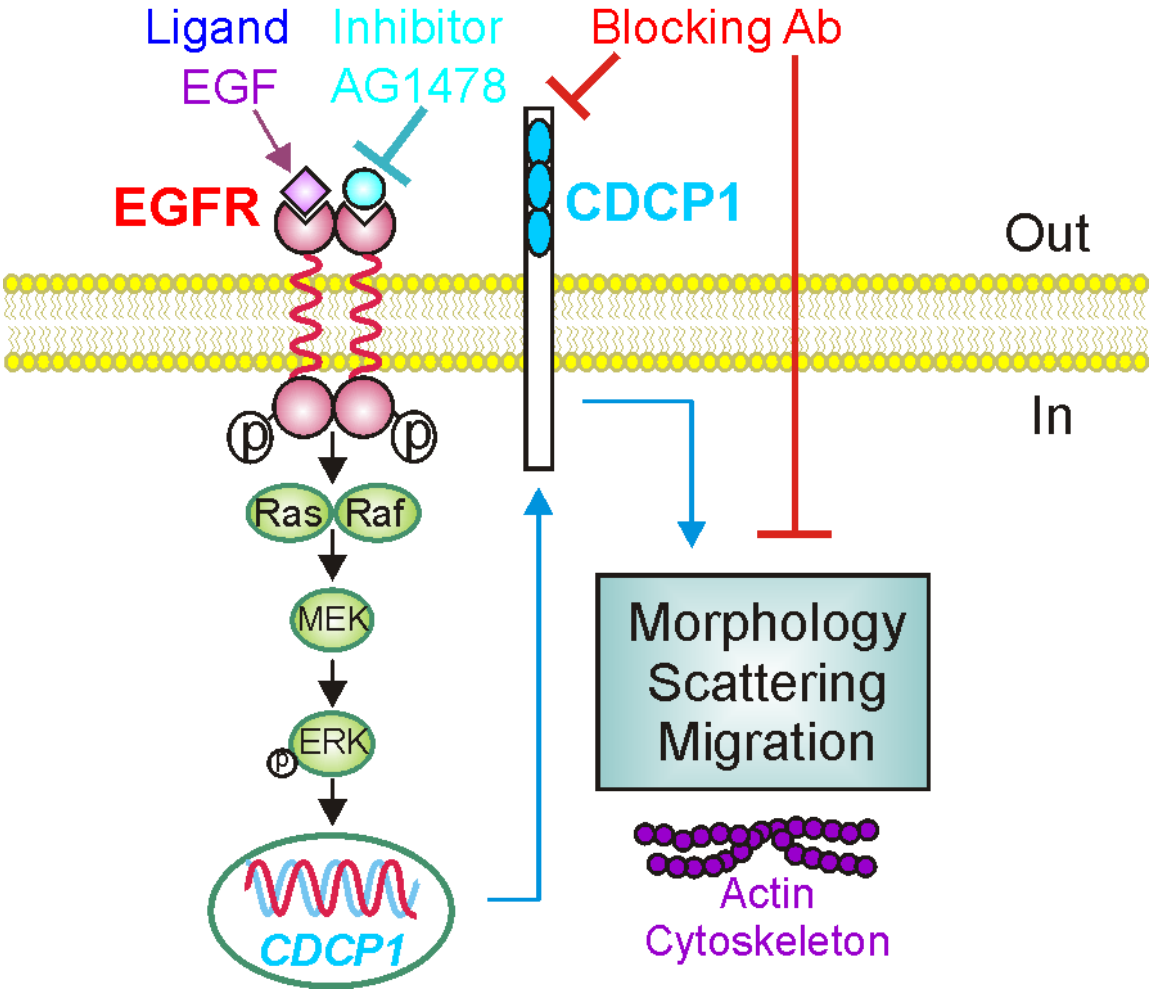
Ligand
EGF
Inhibitor
AG1478
Blocking Ab
EGFR
CDCP1
Out
In
P
P
Ras
Raf
MEK
ERK
P
CDCP1
Morphology
Scattering
Migration
Actin
Cytoskeleton